Eur. Phys. J. C 49, 143–148 (2007)
DOI 10.1140/epjc/s10052-006-0113-6

THE EUROPEAN PHYSICAL JOURNAL C

Regular Article – Experimental Physics

Investigation of the ALICE muon forward spectrometer performances for upsilon measurement

F. Guérin[a] for the ALICE Collaboration

Laboratoire de Physique Corpusculaire – CNRS/IN2P3, Université Blaise Pascal, 63177 Aubiére Cedex, France

Received: 4 August 2006 /
Published online: 16 November 2006 –

Abstract. ALICE (A Large Ion Collider Experiment) is the LHC detector dedicated to the study of nucleus–nucleus collisions, in which the formation of the quark–gluon plasma (QGP) is expected. Heavy quarkonia, especially the Upsilon states, are relevant for studying the QGP since they provide an essential probe of the earliest and hottest stages of heavy ion collisions. They will be measured via their dimuon decay channel in ALICE in the muon spectrometer. The muon spectrometer performance has been studied in simulations, the results will be presented with emphasis on the trigger efficiency and rate in Pb–Pb collisions. The expected yields of Upsilon states will be extracted from a simulation based on a global fit of the dimuon mass spectra for different collision centralities.

1 Introduction

ALICE [1] is the LHC detector dedicated to the study of nucleus–nucleus collisions. The main goal of ALICE is to characterize a deconfined state of nuclear matter called the quark–gluon plasma (QGP), predicted by the QCD theory (quantum chromodynamics). Heavy quarkonia, produced in heavy ion collisions, represent an essential tool to study the nature of the nuclear medium since their yields are sensitive to QGP formation. In a deconfined medium heavy quarkonia production is expected to be sensitive to color screening [2, 3]. Another observable sensitive to the QGP phase is the energy loss of heavy quarks (charm and beauty) [4, 5] by gluon radiation.

ALICE consists of a central barrel ($|\eta| < 0.9$) and a forward muon spectrometer ($-4 < \eta < -2.5$). ALICE has been designed to work in an environment with large particle multiplicities (up to 8000 charged particles per unit of rapidity at mid-rapidity for the most central Pb–Pb collisions). The muon spectrometer (Fig. 1) has been designed to measure and to separate the upsilon states and psi states: the mass resolution is about 100 MeV/c^2 at the Υ mass and 70 MeV/c^2 at the J/ψ mass. In the muon spectrometer the quarkonia will be detected via their dimuon decay channel in the angular acceptance of $(2°, 9°)$: the geometrical acceptance for quarkonia is of the order of 5%. The muon spectrometer can be divided in four parts, as can be seen in Fig. 1: the small angle absorber and the front absorber which reduce the background in the spectrometer, the tracking chambers and the dipole magnet which allow measuring the particle momentum, the muon filter which further reduces the background on the trigger chambers and the trigger system which selects events with muon candidates above a given transverse momentum (p_{T}).

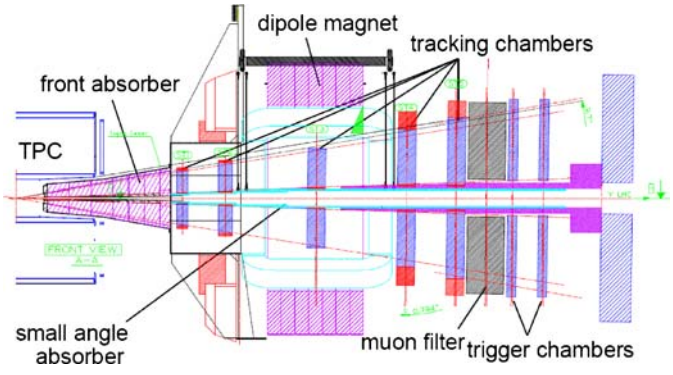

Fig. 1. Layout of the ALICE muon spectrometer

2 Muon trigger performances

In this section, after a brief description of the trigger algorithm, the expected muon trigger efficiency and expected rates in Pb–Pb collisions at $\sqrt{s_{NN}} = 5.5$ TeV are presented.

2.1 Trigger algorithm

The muon trigger is based on single gap RPCs (resistive plate chambers). The trigger algorithm is performed by means of dedicated electronics [6]. Basically, tracks pointing approximately back to the primary interaction vertex are searched for, using the information provided by four

[a] e-mail: fabien.guerin@clermont.in2p3.fr

RPC detector planes. Signals in at least 3 out of 4 detector planes are required to define a track. In the bending plane, the track deviation relative to a particle with infinite momentum is computed. Subsequent cuts on the value of this deviation, performed by means of lookup table, allow rejecting low p_{T} particles. The muon trigger performs two trigger p_{T} cuts. The first one, at $p_{\mathrm{T}} \sim 1\,\mathrm{GeV}/c$, called low p_{T} cut, is optimized for J/ψ physics. The second one, at $p_{\mathrm{T}} \sim 2\,\mathrm{GeV}/c$, called high p_{T} cut, is optimized for Υ physics [7].

2.2 Muon sources

The expected main sources of muons, quarkonia states and physics continuum (pions, kaons, charm and beauty hadrons) are generated by Monte Carlo according to parameterizations, corresponding to the Pb–Pb collision system. The transverse momentum distribution of quarkonia are extrapolated to LHC energies from CDF measurements, according to the procedure outlined in [8], and the rapidity distributions are obtained from the color evaporation model (CEM) [9]. The correlated/uncorrelated open charm and open beauty have been generated using PYTHIA [10, 11]. The PYTHIA parameters have been tuned to reproduce the kinematical distributions of heavy quarks from pQCD calculations at next to leading order [12, 13]. For muons from pion and kaon decays, the transverse momentum and the pseudo-rapidity distributions have been generated according to parameterizations [14, 15] of HIJING events [16] assuming a charged particle multiplicity per unit of pseudo-rapidity at mid-pseudo-rapidity $\mathrm{d}N_{\mathrm{ch}}/\mathrm{d}\eta|_{\eta=0} = 6000$. The whole analysis is performed in the AliRoot framework [17] based on ROOT [18] for simulation, reconstruction and analysis in the ALICE experiment.

2.3 Trigger efficiency

The trigger efficiency is defined as the ratio of the number of muons satisfying a given trigger p_{T} cut to the number of so-called "triggerable" muons. A "triggerable" muon must fire at least 3 out of the 4 possible trigger planes. With such a definition, acceptance (geometrical cuts and absorption of low energy particles) effects cancel out. The expected muon trigger efficiency for quarkonia and physics continuum is reported in Table 1, for low and high p_{T} cuts. The trigger system rejects an important fraction of muons from pions and kaons which are the main contribution to the background (trigger rate). With the low (high) p_{T} cut, the trigger efficiency is high for J/ψ (Υ).

2.4 Trigger rates

The trigger rate, for a given p_{T} cut, is given by:

$$f_{\mathrm{cut}}^{\mathrm{trig}} = f_{\mathrm{reac}} P_{\mathrm{cut}}^{\mathrm{trig}}\,, \tag{1}$$

Table 1. Muon trigger efficiency for "triggerable" muons from quarkonia (φ, J/ψ, Υ) and physics continuum (π/K for pions and kaons, charm and beauty hadrons), for low and high p_{T} cuts

	Quarkonia			Physics continuum		
	φ	J/ψ	Υ	π/K	charm	beauty
low p_{T} cut	13%	71%	97%	13%	27%	70%
high p_{T} cut	2%	22%	88%	4%	8%	36%

where f_{reac} is the mean collision rate and $P_{\mathrm{cut}}^{\mathrm{trig}}$ is the trigger probability (dimuon or single muon). In the centrality range ($b_1 < b < b_2$), f_{reac} is given by:

$$f_{\mathrm{reac}} = \bar{\mathcal{L}}\pi\left(b_2^2 - b_1^2\right), \tag{2}$$

where $\bar{\mathcal{L}}$ is the mean luminosity. For the nominal luminosity $\bar{\mathcal{L}} = 5 \times 10^{26}\,\mathrm{cm}^{-2}\,\mathrm{s}^{-1}$ [1], $f_{\mathrm{reac}} \sim 4000\,\mathrm{Hz}$ for Pb–Pb minimum bias collisions.

For each centrality class, pions, kaons, charm and beauty hadrons are generated according to their respective multiplicity (Poisson distribution around their mean value). The centrality dependence of the multiplicity, for each source, is assumed to be proportional to the number of hard processes[1]. We used the Glauber model to calculate this centrality dependence. The mean multiplicity of muons and dimuons, above a given p_{T} cut, is summarized in Table 2 for central Pb–Pb collisions.

From the trigger response of each event, the impact parameter-integrated unlike-sign dimuon trigger rates as a function of impact parameter are calculated for low and high p_{T} cuts. Figure 2 shows the expected trigger rates as a function of impact parameter for each p_{T} cut. For unlike-sign dimuons the expected trigger rates in minimum bias collisions are $\sim 330\,\mathrm{Hz}$ for low p_{T} cut and $\sim 65\,\mathrm{Hz}$ for high p_{T} cut, to be compared with the collision frequency of 4000 Hz (Table 3). Such event rates fit the bandwidth of ALICE data acquisition system for dimuons [19]. These trigger rates can be compared to the number of quarkonia triggered per second which are about one J/ψ per second and one Υ in one hundred seconds (Table 3).

Table 2. Mean multiplicity for single muons and unlike-sign dimuons above low and high p_{T} cuts in central Pb–Pb collisions

Single muons		Unlike-sign dimuons	
low p_{T} cut	high p_{T} cut	low p_{T} cut	high p_{T} cut
2.09	0.64	1.25	0.16

[1] Simulations have shown that only muons decaying from pions and kaons produced in hard interactions can fire the trigger.

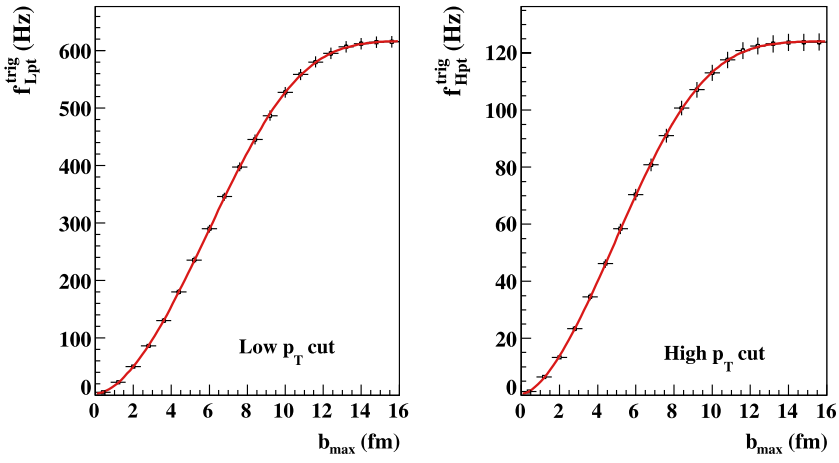

Fig. 2. Impact parameter integrated unlike-sign dimuon trigger rates for low p_{T} (*left*) and high p_{T} (*right*) cuts

Table 3. Unlike-sign dimuon trigger rates and number of quarkonia (J/ψ, Υ) triggered per second in Pb–Pb minimum bias collisions for low and high p_{T} cuts. For comparison, the collision frequency of Pb–Pb minimum bias collisions is indicated

	$f_{\mathrm{coll}} = 4000$ Hz		
	trigger rate	J/ψ	Υ
$f^{\mathrm{trig}}_{\mathrm{Lpt}}$ (Hz)	330	0.85	0.012
$f^{\mathrm{trig}}_{\mathrm{Hpt}}$ (Hz)	65	0.26	0.01

3 Upsilon states yield

In this section, the expected yields of upsilon states in an ALICE Pb–Pb data taking period (10^6 s running time at a luminosity of $5 \times 10^{26}\,\mathrm{cm}^{-2}\,\mathrm{s}^{-1}$) are presented. These yields are extracted, as a function of the collision centrality, from a global fit of the unlike-sign dimuon invariant mass spectra.

3.1 Simulation inputs

In the high mass region ($M_{\mu^+\mu^-} > 4\,\mathrm{GeV}/c^2$), Upsilon states, open charm, open beauty, pions and kaons are the main muon sources. The particle generation is described in Sect. 2.2.

The detector response (tracking and trigger efficiencies, geometrical acceptance) and the detector effects on muon transport (energy loss and momentum smearing) are calculated from parameterizations which depend on the muon phase-space. The mean geometrical acceptance ($\bar{\alpha}_{\mathrm{acc}}$) and the mean efficiency ($\bar{\varepsilon}$), defined as the product of tracking efficiency by trigger efficiency, are reported in Table 4. In this analysis, the trigger high p_{T} cut and an additional p_{T} cut of 1 GeV/c are applied to each muon.

The Upsilon state yields can be studied in five centrality classes as suggested by ZDC (zero degree calorimeter) performance studies [8]. For each component (upsilon states, open charm, open beauty, pions and kaons) and for each centrality class, the unlike-sign dimuon mass spectrum is normalized using the following equation:

$$N^{\mathrm{PbPb}}_{\mu\mu} = f_{\mathrm{coll}}(b) T^{\mathrm{PbPb}}(b) \sigma^{pp} C_{\mathrm{sh}}(b) \mathcal{BR}_{\mu\mu} \alpha_{\mathrm{acc}} \varepsilon \Delta\tau\,, \quad (3)$$

where $T^{\mathrm{PbPb}}(b)$ is the nuclear overlap function for Pb–Pb collisions obtained from the Glauber model [20, 21]. The term $\mathcal{BR}_{\mu\mu}$ represents the dimuon branching ratio for quarkonia or heavy quark pairs. $\Delta\tau$ is the effective acquisition time (10^6 s). The proton–proton cross section σ^{pp} at $\sqrt{s_{NN}} = 5.5$ TeV is calculated from the color evaporation model [8] for upsilon states and from pQCD calculations at next to leading order for open charm and open beauty [13]. The values are summarized in Table 5. The term $C_{\mathrm{sh}}(b)$ is the EKS98 shadowing factor [22] which depends on centrality. The impact parameter dependence of this factor is parameterized [23] as:

$$C_{\mathrm{sh}}(b) = C_{\mathrm{sh}}(0) + (1 - C_{\mathrm{sh}}(0)) \left(\frac{b}{16}\right)^4\,, \quad (4)$$

Table 4. Mean geometrical acceptance relative to 4π ($\bar{\alpha}_{\mathrm{acc}}$) and mean efficiency factor ($\bar{\varepsilon}$) for quarkonia and heavy quark pairs. The efficiency factor is the product of the tracking efficiency ($\varepsilon_{\mathrm{Tk}}$) by the trigger efficiency ($\varepsilon^{\mathrm{Hpt}}_{\mathrm{Tr}}$) for the high p_{T} cut (Hpt). These numbers are obtained from fast simulations in AliRoot framework

	$c\bar{c}$	$b\bar{b}$	Υ	Υ'	Υ''
$\bar{\alpha}_{\mathrm{acc}}$	0.036	0.044	0.05	0.05	0.05
$\bar{\varepsilon} = \bar{\varepsilon}^{\mathrm{Hpt}}_{\mathrm{Tr}} \bar{\varepsilon}_{\mathrm{Tk}}$	0.0018	0.027	0.736	0.746	0.751

Table 5. Cross section (σ_{pp}) in proton–proton collisions and EKS98 shadowing factor ($C_{\mathrm{sh}}(0)$) in central Pb–Pb collisions at $\sqrt{s_{NN}} = 5.5$ TeV for upsilon states and heavy quark pairs

	$c\bar{c}$	$b\bar{b}$	Υ	Υ'	Υ''
σ_{pp} (μb)	6640	210	0.501	0.246	0.100
$C_{\mathrm{sh}}(0)$	0.65	0.84	0.76	0.76	0.76

where the factor $C_{\rm sh}(0)$ represents the shadowing effect in Pb–Pb collisions at $b = 0$ impact parameter. This factor is reported in Table 5 for heavy quarks and Upsilon states. The other terms of (3) have been defined previously in this paper.

3.2 Extraction method of upsilon state yields

After normalization, a histogram is filled with all contributions to the unlike-sign dimuon mass spectrum for each centrality bin. The obtained histogram is shown in Fig. 3 in case of central Pb–Pb collisions, where the contribution of uncorrelated background has been superimposed. Generated statistics being more important than expected statistics, the statistical fluctuations of this spectrum are generated by smearing the content of each bin according to a Poisson distribution. In this study, a perfect subtraction of uncorrelated background is assumed. In this case, the statistical error in each bin of the correlated dimuon mass spectrum is given by the following expression:

$$\sigma_{\rm bin\ cor} = \sqrt{N_{\rm bin\ tot}}\,, \tag{5}$$

where $N_{\rm bin\ tot}$ is the number of entries in each bin of the total mass spectrum (uncorrelated + correlated). After subtraction of uncorrelated background, we extract the upsilon state yields from a global fit of the correlated dimuon mass spectrum with an exponential for the correlated continuum (beauty and charm) and a "modified" Breit–Wigner for the upsilon states. This last function can be written:

$$f(M_{\mu\mu}) = g(M_{\mu\mu})\frac{\Gamma_\Upsilon^2}{\Gamma_\Upsilon^2/4 + (M_{\mu\mu} - M_\Upsilon)^2}\,, \tag{6}$$

where g is a polynomial function with 3 free parameters which takes into account detector effects on muon transport. The mean mass (M_Υ) and mass resolution ($\sigma_\Upsilon = 2.35\Gamma_\Upsilon$) are extracted from the fit. The obtained mass resolution is about 100 MeV/c^2 for each upsilon state (see Fig. 4).

Figure 5 shows the fit of the correlated dimuon mass spectrum and the extracted yields for one month of central Pb–Pb collisions. The yields for Upsilon states and correlated continuum (charm + beauty) correspond to a dimuon mass range $M_{\mu^+\mu^-} > 4\,{\rm GeV}/c^2$. The same method has been applied to extract the Upsilon state yields in other centrality classes and in minimum bias collisions, as shown in Fig. 6. The obtained yields are summarized in Table 6. We note the large statistics for Υ and the separation of the different upsilon states for each centrality bin. For comparison, the generated yields in case of central Pb–Pb collisions are also given in Table 6. One can see that the numbers are very close. The quoted errors on the yields are the statistical errors returned by the fit. The fit stability has been checked successfully by performing 1000 different

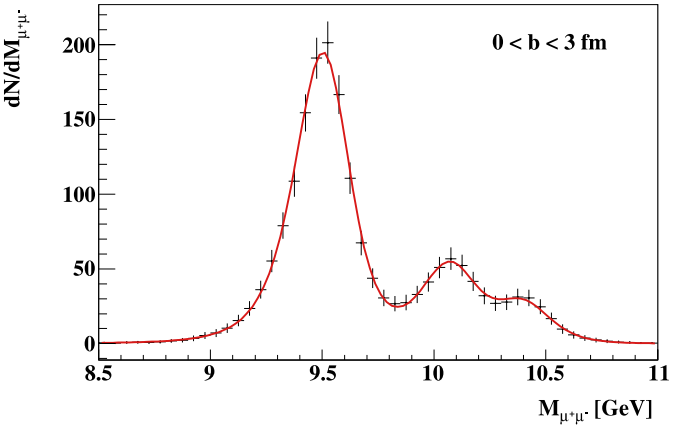

Fig. 4. Fit of the dimuon invariant mass spectrum in Υ mass region for central Pb–Pb collisions without background. The fit function for each upsilon state is defined in text

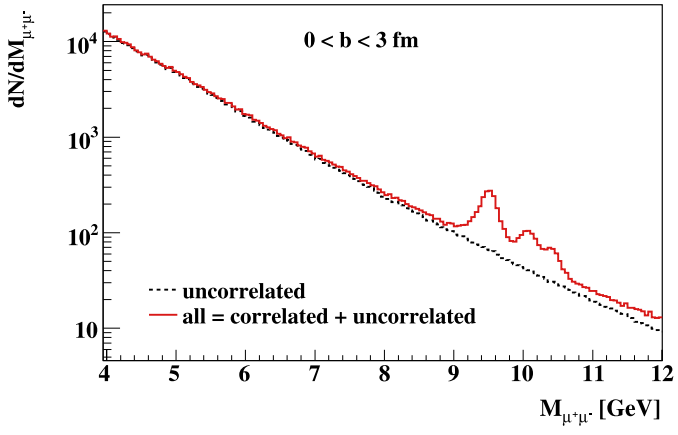

Fig. 3. Unlike-sign total (correlated and uncorrelated) dimuon mass spectrum (*solid line*) and unlike-sign uncorrelated dimuon mass spectrum (*dashed line*). The error bars are not represented. The spectra are normalized to one month of central Pb–Pb collisions

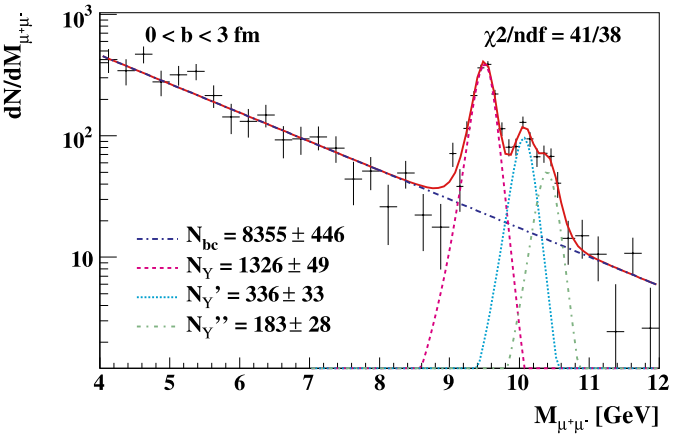

Fig. 5. Unlike-sign correlated dimuon mass spectrum, after subtraction of uncorrelated background. The spectrum is normalized to one month of central Pb–Pb collisions. The upsilon state yields and the continuum are extracted from a global fit of this spectrum

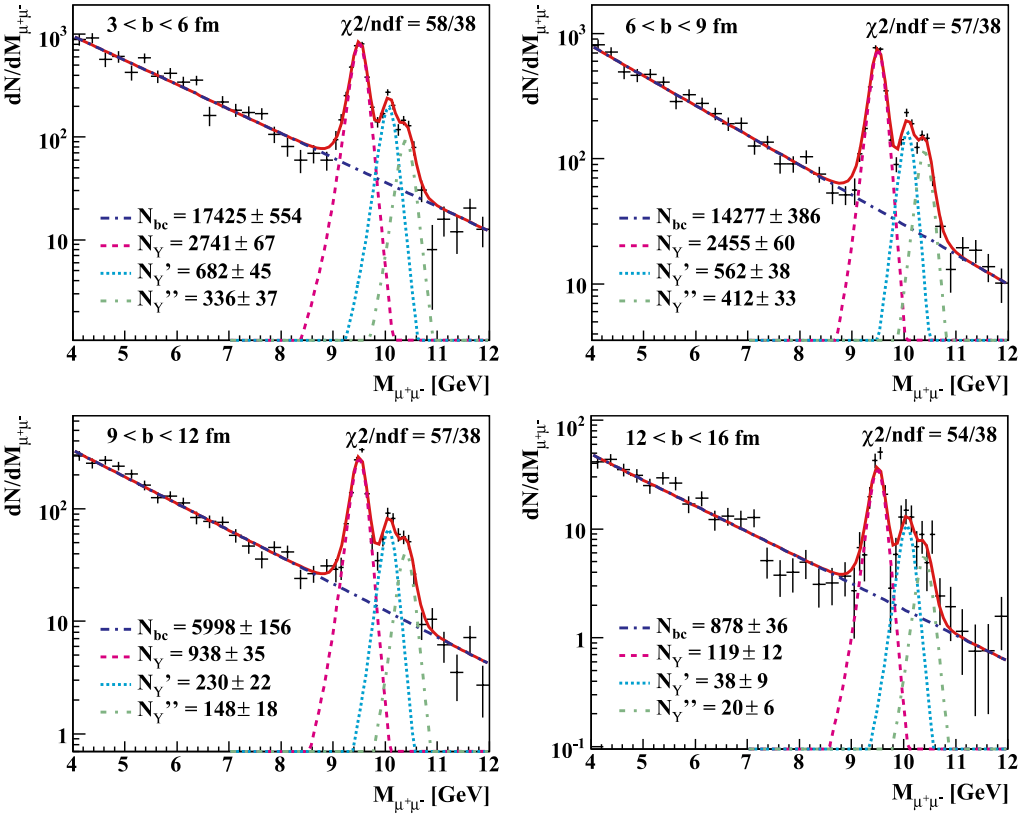

Fig. 6. Unlike-sign correlated dimuon mass spectra and expected yields for one month of Pb–Pb collisions for the other centrality classes

Table 6. Upsilon state yields expected in ALICE muon spectrometer, for five centrality classes and for minimum bias collisions (last line). All yields are for 10^6 s running time with a Pb–Pb luminosity of 5×10^{26} cm^{-2} s^{-1}. For comparison, the generated yields are given in the case of central Pb–Pb collisions (second line)

centrality (fm)	Υ	Υ'	Υ''
0–3	1326 ± 49	336 ± 33	183 ± 28
0–3 (gen.)	1323	351	194
3–6	2741 ± 67	682 ± 45	336 ± 37
6–9	2455 ± 60	562 ± 38	412 ± 33
9–12	938 ± 35	230 ± 22	148 ± 18
12–16	119 ± 12	38 ± 9	20 ± 6
Min. bias	7385 ± 108	1973 ± 73	1064 ± 60

fits with bin-to-bin fluctuations corresponding to different smearing, as described in the beginning of this section.

4 Summary

The study of the trigger performances indicates that, for the low p_{T} cut, the trigger efficiency for "triggerable" J/ψ is around 71% with the unlike-sign dimuon trigger rate of 330 Hz. For the high p_{T} cut, the trigger efficiency for "triggerable" Υ is around 88% with the unlike-sign dimuon trigger rate of 65 Hz. The dimuon trigger rates match the bandwidth of ALICE data acquisition system and the quarkonia efficiency is high. The geometrical acceptance for quarkonia is of the order of 5% and the mass resolution for J/ψ and Υ is about 70 MeV/c^2 and 100 MeV/c^2, respectively.

The upsilon state yields have been extracted from a global fit of the dimuon mass spectra. About 8000 Υ, 2000 Υ' and 1000 Υ'' are expected in one month running for Pb–Pb minimum bias collisions. For each centrality class, the separation of the upsilon states is possible. A large statistics and quite low statistical errors, less than 10%, are obtained. We can thus conclude that Υ physics looks very promising with the ALICE muon spectrometer.

Acknowledgements. Part of this work was supported by the EU Integrated Infrastructure Initiative Hadron-Physics Project under contract number RII3-CT-2004-506078.

References

1. F. Carminati et al., J. Phys. G **30**, 1517 (2004)
2. T. Matsui, H. Satz, Phys. Lett. B **178**, 416 (1986)
3. S. Digal, P. Petreczky, H. Satz, Phys. Rev. D **64**, 094015 (2001)
4. M. Gyulassy, P. Levai, I. Vitev, Nucl. Phys. B **594**, 371 (2001)
5. R. Baier, D. Schiff, B. Zakharov, Ann. Rev. Nucl. Part. Sci. **50**, 37 (2000)
6. G. Blanchard, P. Crochet, P. Dupieux, ALICE-EN-2003-010 (2003)

7. B. Forestier, Ph.D. Thesis (Université Blaise Pascal de Clermont-Ferrand, 2003)
8. ALICE Collaboration, CERN/LHCC 2003-049 (2003)
9. M. Bedjidian et al., hep-ph/0311048
10. R. Guernane, P. Crochet, A. Morsch, E. Vercellin, ALICE-INT-2005-018
11. T. Sjostrand, L. Lonnblad, S. Mrenna, PYTHIA 6.2 Physics and Manual, hep-ph/0108264 (2001)
12. M.L. Mangano, P. Nason, G. Ridolfi, Nucl. Phys. B **273**, 295 (1992)
13. N. Carrer, A. Dainese, ALICE-INT-2003-019, hep-ph/0311225
14. K. Eggert, A. Morsch, ALICE/PHY-95-05 (1995)
15. A. Morsch, ALICE/DIM-96-31 (1996)
16. X.N. Wang, M. Gyulassy, Phys. Rev. D **44**, 3501 (1991)
17. http://alisoft.cern.ch/
18. http://root.cern.ch/
19. F. Guerin, F. Yermia, P. Dupieux, P. Rosnet, ALICE-INT-2006-0002
20. R.J. Glauber, G. Matthiae, Nucl. Phys. B **21**, 135 (1970)
21. R. Vogt, Heavy Ion Phys. **9**, 339 (1999) [nucl-th/9903051]
22. K.J. Eskola, V.J. Kolhinen, C.A. Salgado, Eur. Phys. J. C **9**, 61 (1999)
23. V. Emel'yanov, A. Khodinov, S.R. Klein, R. Vogt, Phys. Rev. C **61**, 044904 (2000)